Mechanism of Native Oat Phytochrome Photoreversion: A Time-Resolved Absorption Investigation†

Eefei Chen,‡ Veniamin N. Lapko,§ James W. Lewis,‡ Pill-Soon Song,§ and David S. Kliger*,‡

Department of Chemistry & Biochemistry, University of California, Santa Cruz, California 95064, and Department of Chemistry and Institute for Cellular and Molecular Photobiology, University of Nebraska, Lincoln, Nebraska 68588

Received September 5, 1995; Revised Manuscript Received November 13, 1995⊗

ABSTRACT: The regulation of plant photomorphogenesis is mediated by the thermal reactions that follow light absorption by the phytochrome photoreceptor. Phytochromes are tetrapyrrolic chromoproteins that exist in two photochromically interconvertible forms, a red light absorbing species, Pr, and a far-red light absorbing form, Pfr. Upon irradiation with 670 nm light, the inactive, red light sensing Pr form is converted to the active Pfr form. Although the forward phototransformation has been studied extensively by several groups using various techniques, the Pfr → Pr photoreversion reaction that occurs upon irradiation with 730 nm light is not as thoroughly characterized. In this study, time-resolved absorption (TROD) spectroscopy is used to examine the intermediate species involved in the phytochrome photoreversion mechanism at 10 °C. Analysis of the TROD data identifies three species with lifetimes of 320 ns, 265 μs, and 5.5 ms. TROD results are described in terms of the simplest parallel and sequential kinetic models. Comparison of intermediate spectra from these mechanisms with those of previously reported species from flash photoreversion and low-temperature studies indicates that Pfr photoreversion follows a sequential pathway that does not share any intermediates with the Pr phototransformation pathway.

Photomorphogenic and developmental processes such as chlorophyll synthesis, seed germination, and flowering are regulated by the phytochrome photoreceptor. Phytochromes may be considered light triggers in that the absorption of specific wavelengths of light, near 730 or 667 nm, renders them inactive (Pr)[1] or active (Pfr), respectively. The structural changes that accompany this reversible photoconversion are believed to control a plant's growth and development and therefore have been the focus of many investigations [for a review, see Quail et al. (1995); Furuya & Song, 1994].

Phytochromes are 121−128 kDa proteins containing an open tetrapyrrole chromophore. The chromophore is connected to the apoprotein through a covalent thioether bond at the cysteine moiety found ∼320 residues from the N-terminus (Lagarias & Rapoport, 1980; Hershey et al., 1985; Rüdiger, 1987). There are at least five members of the phytochrome family: A, B, C, D, and E (Hershey et al., 1985); the experiments reported in this paper were conducted with phytochrome A. Several significant structural differences have been detected between the Pr and Pfr forms. The photoevent that occurs upon excitation of Pr is a *Z,Z,Z* to *Z,Z,E* isomerization at the 15,16-double bond of the chromophore (Rüdiger et al., 1983; Kandori et al., 1992; Hildebrandt et al., 1992; Fodor et al., 1990; Farrens et al., 1989). Results of ultrafast pump−probe spectroscopic studies (Kandori et al., 1992; Savikhin et al., 1993) show that this isomerization is the primary photoprocess, occurring within a few picoseconds. Formation of the *Z,Z,E* configuration leads to a reorientation and relaxation of the Pfr chromophore. The resulting Pfr chromophore is more exposed to the medium than the Pr chromophore (Furuya & Song, 1994; Hahn et al., 1984; Chai et al., 1987; Singh et al., 1989; Vierstra & Quail, 1983). Studies have shown that in Pfr the distance between the N-terminus and the chromophore decreases by 12 Å (Farrens et al., 1992; Parker et al., 1992), and the protein responds with an increase in the N-terminus helicity (Singh et al., 1989; Rüdiger, 1992). The importance of this increase in helicity for the regulation of photomorphogenic processes by Pfr is underscored by the observation that the N-terminus is required for full physiological activity (Cherry et al., 1992; Stockhaus et al., 1992).

The time course of structural changes that occur upon the excitation (Pr → Pfr) of phytochrome has recently been studied using time-resolved circular dichroism (TRCD) and absorption (TROD) techniques in the far-red and far-UV spectral regions (Zhang et al., 1992; Björling et al., 1992; Chen et al., 1993). Results of the far-red TROD investigations show that at 10 °C five intermediates participate in the photoactivation process, lumi-R1 (7.4 μs), lumi-R2 (89.5 μs), meta-Ra1 (7.6 ms), meta-Ra2 (42.4 ms), and meta-Rc (>266 ms), although in more recent studies of this reaction, Braslavsky did not consider the meta-Ra1 species to be a significant intermediate (S. E. Braslavsky, private communication to P.S.S.). The structural changes that accompany the formation and decay of these intermediate species were identified by using TRCD spectroscopy in the far-red region since circular dichroism methods are more

† This work was supported by NIH Grants GM-35158 (D.S.K.) and GM-36956 (P.S.S.) and a University of California President's Postdoctoral Fellowship (E.C.).

* Author to whom correspondence should be addressed.
‡ University of California.
§ University of Nebraska.

⊗ Abstract published in *Advance ACS Abstracts,* January 1, 1996.

[1] Abbreviations: Pr, red light absorbing phytochrome; Pfr, far-red light absorbing phytochrome; TROD, time-resolved optical density (time-resolved absorption); TRCD, time-resolved circular dichroism; Pr → Pfr, phytochrome phototransformation reaction; Pfr → Pr, phytochrome photoreversion reaction; PPB, potassium phosphate buffer; SAR, specific absorbance ratio; FWHM, full-width half-maximum; SVD, singular value decomposition.

0006-2960/96/0435-843$12.00/0

sensitive than absorption methods to chromophore asymmetry induced by the protein environment. The results of far-red TRCD studies indicate that the formation of the early lumi-R intermediates corresponds to chromophore isomerization and that structural changes in these intermediates are localized within the chromophore pocket. After isomerization, a chromophore relaxation step is expected and has been associated with the formation of the meta-Ra1 species (Eilfeld & Rüdiger, 1985). The suggestion that later meta intermediates are responsible for protein structural changes was investigated with far-UV TRCD experiments (Chen et al., 1993), which showed that formation of the final Pfr structure is preceded by at least one detectable protein rearrangement on the millisecond time scale.

The Pfr photoreversion reaction (Pfr → Pr) is also important in maintaining a physiological balance in plant development. Thus far, up to three intermediates, lumi-F, meta-Fa, and meta-Fb, have been detected through low-temperature spectroscopy and flash photoreversion techniques. However, a detailed kinetic scheme of phytochrome photoreversion has not yet been elucidated. Here we report the results of far-red TROD measurements of the Pfr → Pr photoreversion reaction, which reveal three intermediate species with lifetimes of 320 ns, 265 μs, and 5.5 ms. The spectra of these species calculated from a sequential kinetic model for the Pfr → Pr photoreversion are presented and compared to those of the intermediates detected previously. We also discuss the possibility that common intermediates are formed in both Pr → Pfr and Pfr → Pr pathways.

MATERIALS AND METHODS

Phytochrome Purification. *Avena sativa* L., certified Garry oat (Agriculver, Trumansburg, NY) seedlings, were grown in the dark on moist Vermiculite for approximately 3 days at 25 °C and harvested under a green safety light. The seedlings were stored for 1−2 days at 2 °C before use.

Native 124 kDa oat phytochrome A was isolated according to a modification (Lapko & Song, 1995) of the method of Chai et al. (1987). Briefly, fresh oat seedlings (1.3 kg) were ground up using a Waring blender, and particulate matter was removed by centrifugation. Precipitation of nucleic acids, pectins, and acidic proteins with poly(ethylene imine) and subsequent precipitation of phytochrome from the supernatant with ammonium sulfate were performed as described by Vierstra and Quail (1983). The phytochrome containing pellet was homogenized in 50 mM Tris-HCl buffer (pH 7.8) using a glass tissue grinder, and the resulting solution was clarified by centrifugation. Phytochrome from the solution was reprecipitated using 3.3 M ammonium sulfate (50 mL per 100 mL of phytochrome solution). After 15 min of stirring, the phytochrome pellet was collected by centrifugation. The pellet was washed 4−5 times with 100 mM potassium phosphate buffer (PPB) (pH 7.8) using 0.5−0.7 mL of 100 mM PPB per 1 mg of phytochrome for two initial washing steps and volumes half as large for subsequent steps. The pellet was washed additionally with 1.5−2.5 mL of 10 mM PPB (pH 7.8) and finally dissolved in 10 mM PPB using two solubilization steps with a small amount (2−3 mL) of the buffer. The combined phytochrome fraction was irradiated with far-red light and applied to a Toyopearl HW-65S gel filtration column equilibrated with 20 mM Tris-HCl buffer (pH 7.8) containing 0.5 mM EDTA. Specific absorbance ratios (SAR, A_{667}/A_{280}) of ≥1.0 were routinely obtained for freshly purified samples. Sample aliquots of 1−1.2 mL were frozen on dry ice until the experiment.

SDS−PAGE was performed according to the method of Laemmli (1970), employing 7.5% acrylamide. The proteins were stained with Coomassie Brilliant Blue R. A high-range SDS−PAGE standard set (Bio-Rad Laboratories, Richmond, CA) was used for molecular weight determinations. The phytochrome preparations exhibited a single 124 kDa band on SDS−PAGE even when 5 μg of phytochrome was applied.

The absorption spectra of phytochrome solutions were recorded on a Hewlett-Packard 8452A spectrophotometer at 2−4 °C under a green safety light. Phytochrome photoconversions were performed using a fiber optic illuminator (G-09745-00, Cole-Parmer, Niles, IL) with 660 and 730 nm interference filters (02-6603 and 02-7303, Optometrics, Ayer, MA) for the red light and far-red light sources, respectively.

Experimental Protocol. Phytochrome samples were prepared for experiments by dilution into 20 mM Tris-HCl buffer (pH 7.8) containing 0.5 mM EDTA. The final concentration of the solutions was ca. 6 μM to give an OD of ca. 0.6 at 730 nm. The samples had an SAR value of 0.9 or higher and a Pfr to Pr absorbance ratio (A_{730}/A_{667}) greater than 1.40. The slight drop in the SAR value from that of the freshly prepared material results from redissolving frozen phytochrome samples. For each experiment approximately 4−5 mL of sample was circulated with a peristalic pump between an iced sample reservoir and the optical cell. Before the experiment the sample was photoconverted to Pfr by irradiation with a high-intensity CW light (Fiber-Lite Series 180, Dolan-Jenner Industries, Inc.). A red interference filter was used to select 660 nm light. The temperature of the cell was maintained at 10 °C to keep the sample stable.

Photoconversion of phytochrome was initiated with 6−8 mJ pulses of 730 nm laser light [7 ns, full-width half-maximum (FWHM)] generated by a Quanta Ray DCR-2 Nd:YAG pumped dye laser (Spectra-Physics, Mountain View, CA). Transient spectral changes resulting from photoexcitation were probed with a xenon flash lamp source. The probe beam polarization was set at 54.7° (magic angle) relative to the laser light polarization, so that optical artifacts arising from photoselection and protein rotational diffusion did not interfere with the results. A 360 nm cutoff filter (O-51, Corning Glass Works, Corning, NY) and a true pink or smokey pink LEE filter (Musson, Santa Clara, CA) were used to avoid artifacts due to second-order light and to obtain a smooth broadband continuum across the 400−900 nm spectral region. Depending upon the flow cell path lengths, 2 or 10 mm, the excitation beam overlapped the probe beam at an angle of 15° or 90°, respectively. The probe beam was focused into a Monospec 27 spectrograph (Thermo Jarrell Ash, Franklin, MA) equipped with a 500 μm slit and a 150 grooves/mm grating and collected with a red-sensitive, gated optical multichannel analyzer detector (OMA, Model 1420RT, EG&G PARC, Princeton, NJ). The OMA detector image intensifier was gated by a pulse amplifier (Model 1304 EG&G PARC or Model AVL-2A-PS-W-N, Avtech Electro Systems, Ottawa, Canada), and the signal was read with a detector interface (Model 1461 EG&G PARC) that was controlled by an IBM-compatible microcomputer. Timing

between laser, probe light, and detector gate was synchronized by a four-channel digital delay generator (DG535, Stanford Research Systems, Sunnyvale, CA).

Data were collected at logarithmic delay times after photoexcitation, with approximately 10 points in each time decade from 50 ns to 1 s, followed by measurements at 2, 4, 8, and 16 s. Each experiment typically involved 16 averaged scans at each time point with a 10 s delay between each laser event. During this 10 s period the solution was flowed out of the pump−probe path and the solutions in the flow cell and the sample reservoir were irradiated with high-intensity 660 nm CW light. The sample was not flowed during the delay between excitation and data collection. These steps ensured that the laser excited pure Pfr. The integrity and concentrations of the samples before and after experiments were determined by optical spectra measured with an IBM 9420 UV−visible spectrophotometer. Any reused sample was first centrifuged for 20 min at 16 000 rpm (Sorvall RC-2, SS-34 rotor, DuPont, Wilmington, DE).

Data Analysis. Difference TROD data were analyzed by using singular value decomposition (SVD) and global analysis methods. These methods have been described in detail elsewhere (Zhang et al., 1992; Henry & Hofrichter, 1992; Goldbeck & Kliger, 1993) and will be discussed only briefly here. SVD is a matrix technique that identifies the minimum number of independent species required to describe the spectral variations in the data and allows experimental noise to be discarded. In a series of unimolecular photolysis reactions where N intermediates are spectrally distinguishable, the time evolution of the intermediates can be probed with the spectral changes that occur after photolysis. SVD analysis decomposes the TROD data matrix (**A**) into mathematically independent spectral (**U**) and temporal (**V**, **V′** is the transpose of **V**) components that are weighted with singular values (**S**) according to the importance to the data:

$$\mathbf{A} = \mathbf{USV}' \tag{1}$$

The temporal behavior of spectral intermediates in the data may be investigated with global kinetic analysis, where the data is fit to a product of time (**T**) and spectral (**B**) functions:

$$\mathbf{A} = \mathbf{BT} \tag{2}$$

The time decay of the concentration of each intermediate to other intermediates or the final product can be described by first-order linear differential equations. Solution of these equations depends on the rate constants of the decay process, as well as on how the intermediates are derived from one another. The concentrations of the intermediates at time t can be written as

$$\mathbf{C} = C_0\mathbf{KT} \tag{3}$$

where C_0 is the concentration of the photolyzed species at $t = 0$, $\mathbf{C} = \{C_1(t), C_2(t), ..., C_N(t), C_{N+1}(t)\}'$, and **K** is an $(N + 1) \times (N + 1)$ matrix that is determined by the reaction mechanism and the apparent rate constants k_1, k_2, k_3, ..., k_N. For TROD measurements that involve m wavelengths and n delay times after photolysis, the difference absorption data can be expressed in matrix form, using eq 3, as a function of difference extinction coefficients of the intermediates and final product relative to the unphotolyzed species and the concentration of the intermediates and final product:

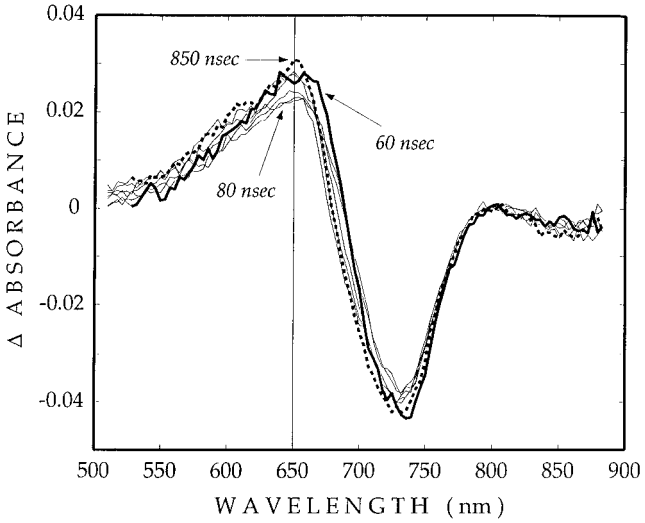

FIGURE 1: TROD difference spectra of $A(t)$-Pfr. The spectra represent a typical data set with 16 averaged scans collected at times between 60 and 850 ns after photoconversion is initiated. The sample was prepared in 20 mM Tris-HCl buffer (pH 7.8) containing 0.5 mM EDTA. Pfr was irradiated with 6−8 mJ of 730 nm laser light. Laser pulses were separated by 10 s, during which Pfr was reformed by 660 nm CW illumination of the cell window and the sample reservoir. This time regime is characterized by a decrease in absorbance at 650 nm from 60 to 80 ns, followed by a gradual increase back to the initial absorbance value from 80 to 850 ns. There is also an 11 nm hypsochromic shift from 686 to 675 nm.

$$\mathbf{A}(\lambda,t) = \epsilon(\lambda)\mathbf{C}(t) = C_0\epsilon(\lambda)\mathbf{KT}(t) \tag{4}$$

The goal of TROD data analysis using global kinetic methods is to identify the intermediate spectra (ϵ) and the corresponding decay rate constants (**T**), as well as the reaction mechanism (**K**) from the raw kinetic data (**A**). When **B**, the spectral components or "*b*-spectra", is defined as $C_0\epsilon(\lambda)\mathbf{K}$, the raw data can be decomposed into spectral and temporal components as shown in eq 2. SVD and global analysis were performed by using the mathematical software package Matlab (Pro-Matlab, The Math Works, Inc., South Natick, MA).

RESULTS

The time dependent difference ($A(t)$-Pfr) absorption spectra of Pr formation from Pfr intermediates are shown in Figures 1−3. In a typical data set, the Pfr → Pr photoconversion was probed from 60 ns to 8 s after laser excitation. For different data sets, each spectrum is an average of either 8 or 16 scans. The peak in the difference spectrum, ca. 664 nm, is near the Pr absorption maximum, and the negative absorption at ca. 730 nm corresponds to the disappearance of Pfr. Figure 1 shows the $A(t)$-Pfr difference spectrum that correspond to time delays between 60 and 850 ns after the initial photoevent. The time dependence of these spectra shows a decrease in absorbance at 650 nm from 60 to 80 ns and then a gradual increase back to the initial absorbance value from 80 to 850 ns. A second feature is an 11 nm blue shift of the zero absorption point from 686 to 675 nm as the spectra progress from 60 to 850 ns after photoconversion. In Figure 2, the spectra are followed from 2.5 to 800 μs after photoconversion. The major spectral evolution is found in the positive absorption band where the maximum absorp-

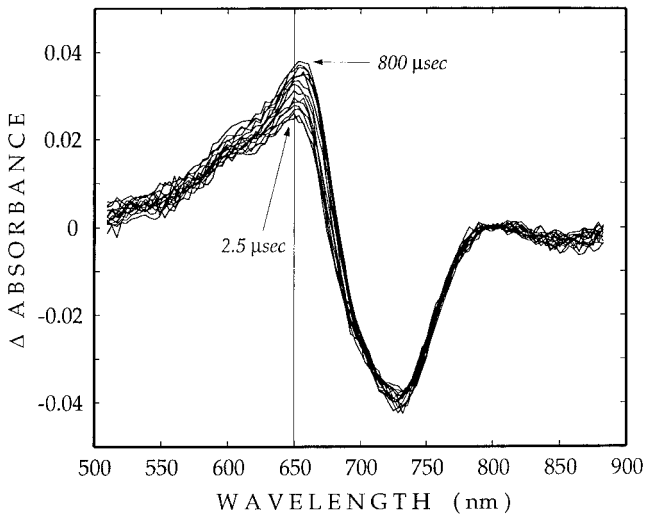

FIGURE 2: TROD difference spectra of $A(t)$-Pfr. These difference spectra were collected from 2.5 to 800 μs after the initiation of phytochrome photoconversion. A small bathochromic shift of the absorption maximum is observable in this time region near 650 nm, as is an increase in the positive absorption from 2.5 to 800 μs. See the legend to Figure 1 for experimental conditions.

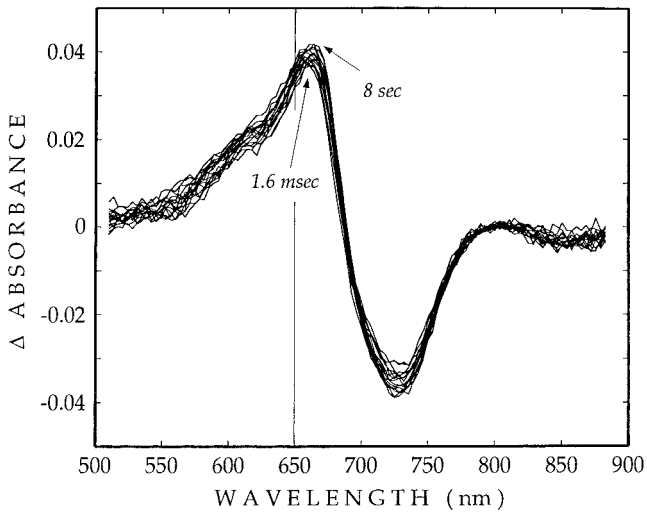

FIGURE 3: TROD difference spectra of $A(t)$-Pfr. Data collected between 1.6 ms and 8 s show few changes as phytochrome photoconversion reaches the final stage, where Pfr is completely transformed to Pr, and the absorption maximum is found at 664 nm. See the legend to Figure 1 for experimental conditions.

tion increases as a function of time delay. The growth of this absorption band is accompanied by a bathochromic shift of the absorption maximum from 650 to 656 nm. Figure 3 shows the spectral evolution as the photoconversion reaches the final stages (1.6 ms to 8 s), where the difference spectrum represents full conversion of Pfr to Pr.

A semilog plot (Figure 4A) of the **S** matrix diagonal elements shows the relative magnitudes of each singular value determined by SVD analysis. SVD decomposes the TROD data into mathematically independent spectral and temporal components, where the significance of each component to the data is indicated by the magnitude of its singular value. The straight line in Figure 4A indicates the pattern of elements expected from random noise. Therefore, this plot suggests that up to four spectrally significant intermediates are present in the photoreversion of Pfr to Pr. Comparison of residual spectra resulting from fitting data to one, two, and three exponentials indicates that the data are best fit with three transient species. Attempts to fit the data to a fourth exponential gave either irreproducible lifetimes or only three lifetime values. Since minor pulse-to-pulse variation of the probe source intensity causes random offsets in spectra, the fourth minor component may arise from the fitting of these offsets. The significant spectral components, or *b*-spectra, calculated for a three-exponential process with lifetimes of 320 $\pm$ 40 ns, 265 $\pm$ 90 μs, and 5.5 $\pm$ 0.5 ms are shown in Figure 4B. They are identified as lumi-F (320 ns), meta-Fa (265 μs), and meta-Fb (5.5 ms) in accordance with terminology introduced by Spruit and Kendrick (1977). Identification of the intermediates was based on spectral similarities to those reported previously.

SVD and global analysis extract information on the apparent rate constants, but these are independent of any specific kinetic models. To calculate true intermediate spectra and the corresponding microscopic rate constants, it is necessary to test different kinetic models. The phytochrome photoreversion mechanisms presented in the following sections are the simplest sequential and parallel models.

The Simplest Parallel Model. The *b*-spectra (Figure 4B) calculated from SVD and global analysis directly correspond

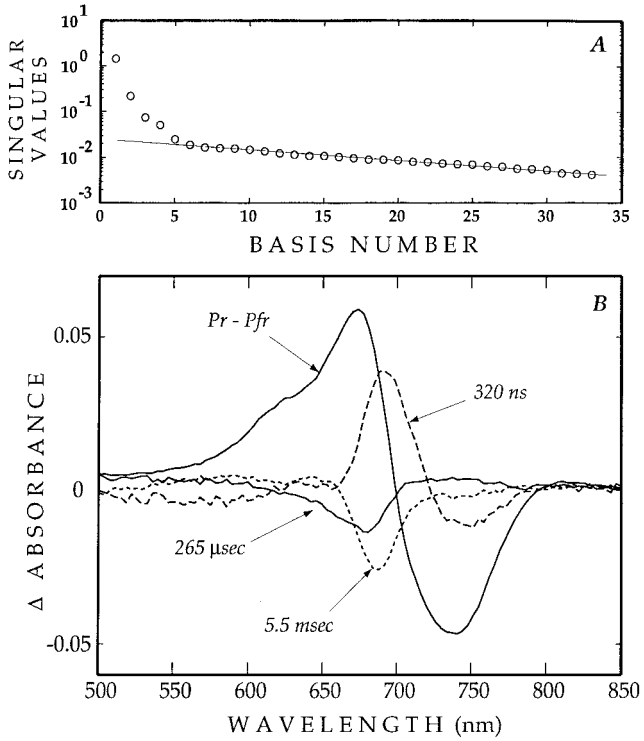

FIGURE 4: SVD and global analysis of TROD difference data. (A) The diagonal elements of the **S** matrix generated by SVD analysis give an estimate of the relative contributions of the mathematically independent components to the data. A semilog plot of the magnitude of each diagonal element shows the presence of up to four spectrally significant intermediates in the photoconversion mechanism. The line through the data represents the behavior of components arising from noise, showing that three or four elements clearly lie outside of the experimental noise. (B) TROD data are best fit to three kinetic processes. Each b-spectrum calculated from global analysis is associated with a lifetime: 320 $\pm$ 40 ns (— —), 265 $\pm$ 90 μs (—), and 5.5 $\pm$ 0.5 ms (- - -). The last spectrum represents the fully converted Pr−Pfr difference spectrum (—).

to the intermediate difference spectra based on the simplest parallel kinetic model:

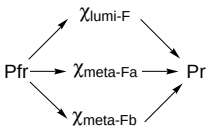

Figure 5 shows the intermediate spectra calculated by adding 33% of the Pfr spectrum to each of the *b*-spectra shown in Figure 4B. The pure Pfr spectrum was first corrected for the 13% phototransformation yield of Pr (664 nm), which was calculated by normalizing the difference spectrum of steady state Pr−Pfr to the *A*(*t*)-Pfr TROD spectrum measured at $t = 1$ s. The spectrum of each intermediate is bathochromically shifted from the absorbance peak of 664 nm for Pr. Lumi-F is distinguished spectrally by a large absorbance band centered at 681 nm, a shoulder at ca. 723 nm, and a small band at ca. 630 nm, while meta-Fb exhibits a broad band with a maximum at 725 nm, a small absorbance at 643 nm, and a negative feature at 676 nm. Meta-Fa is characterized by a negative absorbance at 668 nm and a positive absorbance maximum at 718 nm. Variations of the fraction of each intermediate present generate spectra where at least one intermediate spectrum exhibits either a negative absorption feature or multiple bands.

An Unbranched Sequential Model.

An unbranched sequential model is characterized by distinct intermediate species that decay from one to another, with no reversibility at any step. The difference spectra of intermediate species, $I(\lambda)-\mathrm{Pfr}(\lambda)$, corresponding to a sequential model were calculated according to eqs 1 and 2 and are shown in Figure 6A. The absolute absorption spectra of these intermediates (Figure 6B) were obtained by adding a steady state spectrum of pure Pfr back to the intermediate difference spectra. The first species detected, lumi-F (320 ns), has an absorption maximum (670 nm) that is bathochromically shifted from that of pure Pr (664 nm). Later intermediates are hypsochromically shifted to 656 nm for meta-Fa (265 μs) and 660 nm for meta-Fb (5.5 ms).

Pfr → lumi-F → meta-Fa → meta-Fb → Pr
320 ns 265 μs 5.5 ms
730 nm 670 nm 656 nm 660 nm 664 nm

DISCUSSION

TROD studies have detected three intermediate species, lumi-F, meta-Fa, and meta-Fb, in the Pfr → Pr photoreversion reaction. The lifetimes associated with these species are 320 ns, 265 μs, and 5.5 ms, respectively. We interpret the data according to the simplest sequential and parallel pathways that are consistent with the results of global analysis of the TROD data, as well as with the results of previous flash photoconversion and low-temperature studies. As seen here, this analysis suggests that a sequential mechanism provides a more reasonable explanation of the data available to date.

Table 1 compares the absorption maxima of the intermediates detected in the Pfr → Pr reaction from the present TROD studies to those measured with low-temperature and flash photoreversion methods. Intermediate species from different studies are identified according to the nomenclature chosen by each of the authors. These species are compared to those observed in TROD studies of the forward Pr → Pfr reaction by Zhang et al. (1992) since it is the most recently published

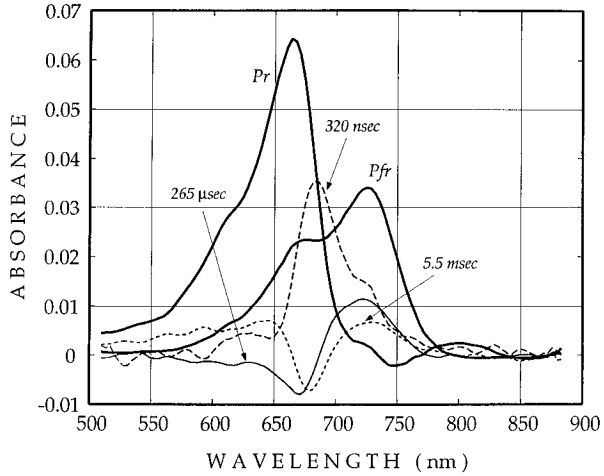

FIGURE 5: Intermediate species for a simple parallel Pfr → Pr mechanism. Addition of a spectrum of Pfr (bold solid line) to the b-spectra in Figure 4B, which are calculated by global analysis for the simplest parallel model, gives spectra for the intermediate species. Lumi-F (− −, 320 ns) shows two absorption bands at 723 and 681 nm, which are bathochromically shifted relative to that for Pr (bold solid line, 664 nm), and a small hypsochromic band centered around 630 nm. Meta-Fa (—, 265 μs) and meta-Fb (- - -, 5.5 ms) both exhibit an absorption band around 720 nm, as well as negative absorption bands at 668 and 676 nm, respectively. Meta-Fb also exhibits a positive feature at 643 nm.

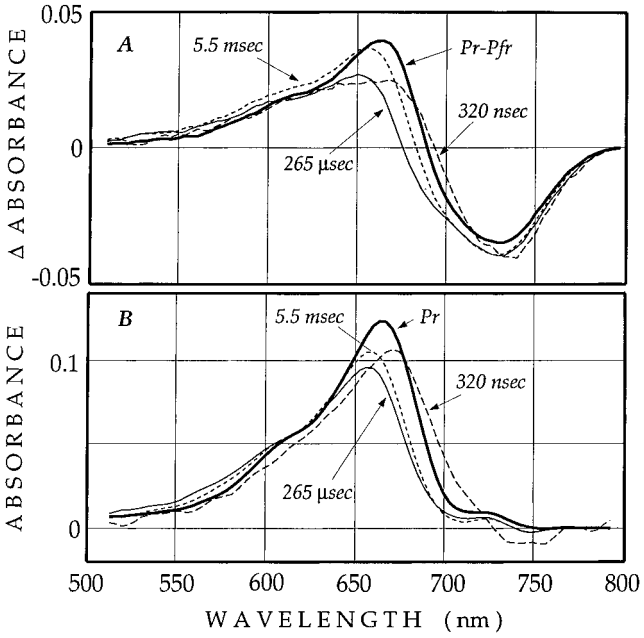

FIGURE 6: Spectra of intermediate species for an unbranched sequential Pfr → Pr model. (A) Difference spectra of intermediate species, $I(\lambda)-\mathrm{Pfr}(\lambda)$, are calculated for a sequential Pfr → Pr kinetic model (320 ns, − −; 265 μs, —; 5.5 ms, - - -). They are compared to the fully transformed Pr−Pfr spectrum (—). The spectra shown are averages of three data sets. (B) Absorption spectra of the transient species are calculated by adding a steady state spectrum of Pfr to the difference spectra in part A after the spectrum of Pfr is normalized to the 13% Pr phototransformation yield. The absorption maxima of the species are found at 670 (lumi-F, 320 ns, − −), 656 (meta-Fa, 265 μs, —), 660 (meta-Fb, 5.5 ms, - - -), and then finally 664 nm, which is characteristic of Pr (—).

TROD study. However, as noted earlier, the significance of the meta-Ra1 intermediate has recently been questioned by Braslavsky (private communication to P.S.S.).

A parallel reaction mechanism can arise from the branching of Pfr → Pr pathways in the process of photoconversion

Table 1: Intermediate Species of Phytochrome Phototransformation Pathways

***Pr*→**						**→*Pfr***
	lumi-R1	***lumi-R2***	***meta-Ra1***	***meta-Ra2***	***meta-Rac***	Zhang et al. (1992)
	692 nm	687 nm	668 nm	733 nm	737 nm	
	7.4 μs	89.5 μs	7.6 ms	42.4 ms	>266 ms	
Pfr →						**→*Pr***
	low temperature					
			A			Burke et al. (1972)
			660 nm			
		***FR*$_{660}$**	***FR′***			Pratt and Butler (1968)
		660 nm	660 nm			
		lumi-F	***meta-F***			Eilfeld and Rüdiger (1985)
		673 nm	660 nm			
		lumi-F	***meta-Fa***	***meta-Fb***		Spruit and Kendrick (1975)[a]
	flash photoreversion					
			***fr*$_1$**	***fr*$_2$**		Linschitz et al. (1966)
			660 nm	660 nm		
			1 ms	5.9 ms		
		lumi-F	***meta-Fa***	***meta-Fb***		this study, parallel model
		681, 718 nm	668, 718 nm	676, 725 nm		
		670 nm	656 nm	660 nm		this study, sequential model
		320 ns	265 μs	5.5 ms		

[a] These studies were performed with fresh or freeze-dried tissues and showed varying wavelengths as a function of irradiation and detection temperatures.

or from inhomogeneities of the phytochrome samples. The latter possibility may be ruled out because phytochrome isolation methods can now prepare highly purified and undegraded samples. Furthermore, the reproducibility of the shapes of the *b*-spectra and corresponding amplitudes suggests a high level of sample homogeneity (or at least invariant inhomogeneity). Examination of intermediate spectra for a simple parallel kinetic model (Figure 5) raises two strong arguments against this type of mechanism. First, calculations of intermediate spectra for various fractional combinations of lumi-F, meta-Fa, and meta-Fb generate at least one spectrum for each combination that has a negative absorption feature. Second, fractions of meta-Fb or meta-Fa above 10% give spectra with multiple absorption bands. These multiple bands indicate that complex interactions occur upon photoisomerization of the phytochrome chromophore, which is not suggested by the spectra of pure Pr and Pfr. These inconsistencies render a simple parallel mechanism an unlikely reaction pathway for the decay of lumi-F, meta-Fa, and meta-Fb to Pr. Comparison of absorption maxima for these intermediate spectra with those previously reported shows few similarities (Table 1). There are no multiple absorbances or wavelength maxima shared between intermediates, and there is little commonality in the wavelength positions of the major absorption bands. Furthermore, the intermediates observed in the Pfr → Pr mechanism from previous studies (Table 1) have largely been discussed in terms of a sequential kinetic model.

Calculation of intermediate spectra based on a sequential kinetic model generates species that are found at 670 (lumi-F), 656 (meta-Fa), and 660 nm (meta-Fb) before the formation of Pr (664 nm) (Table 1). The absolute spectra of these transient species (Figure 6B) do not contain multiple peaks or extraordinarily broad features that might indicate equilibrium between intermediates on this time scale. The spectra of sequential intermediates detected by TROD experiments resemble spectra reported by Eilfeld and Rüdiger (1985, see Figure 4) and difference spectra measured by Linschitz et al. (1966, see Figure 10). Such similarities are significant considering the differences in techniques (low-temperature and flash photoreversion) and samples (60 versus 124 kDa), which would likely produce different spectra should either a parallel or sequential model with back-reactions prevail. The observed similarities support an unbranched, sequential model for Pfr phototransformation. Therefore, the following comparison will focus on those identified according to such a mechanism. An exact correlation between spectra is not expected because of differences in techniques, as well as samples. The differences in the absorption maxima of the intermediates (Table 1) are consistent with the bathochromic shifts observed in low temperature studies of visual pigments (Ono et al., 1986). Additionally, improvements in sample preparation methods that now generate full length 124 kDa phytochrome in contrast with partially degraded samples may explain some of the discrepancies noted in Table 1.

Direct comparison of the processes observed here is only possible with flash photoreversion studies by Linschitz et al. (1966). In single-wavelength flash experiments at 0 °C, the Pfr → Pr reaction was studied from 100 μs to 10 ms after irradiation with an oxygen flash lamp source and a 704 nm cutoff filter. The similarities in the difference absorption spectra (Linschitz et al., 1966) and lifetimes indicate that the reported fr_2 and fr_1 are meta-Fb and meta-Fa, respectively, from these TROD studies. The lifetimes measured for fr_1 and fr_2 are slightly longer, at 1 and 5.9 ms, respectively, than those detected in the TROD data. The longer lifetimes may be due to measurements at 273 K, in contrast to our studies at 283 K, or due to the use of a partially degraded sample versus the 124 kDa phytochrome. Both fr_1 and fr_2 have absorption maxima at 660 nm, while meta-Fa is found at 656 nm and meta-Fb at 660 nm. The difference in wavelength maxima between fr_1 and meta-Fb may be due to differences in the sample and due to wavelength resolution limitations that arise from single-wavelength detection methods, as opposed to multichannel detection techniques used in these TROD studies.

Lumi-F is not expected from these flash photoreversion studies since the apparatus was limited to time regions slower than 100 μs after photoexcitation. However, it was previ-

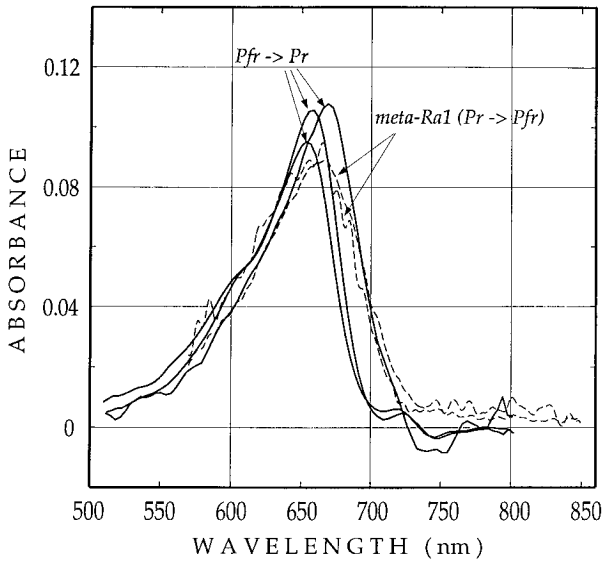

FIGURE 7: Comparison of lumi-F, meta-Fa, and meta-Fb with meta-Ra1 from the Pr → Pfr reaction. The meta-Ra1 species measured in the Pr → Pfr reaction (- - -, λ_{max} = 668 nm) has an absorption maximum similar to those of lumi-F, meta-Fa, and meta-Fb (—) in Pfr → Pr. Meta-Ra1 may be a combination of lumi-F with meta-Fa and/or meta-Fb. When normalized to the absorbance of lumi-F in Figure 6B (data not shown), meta-Ra1 shares the blue edge of the meta-Fa band and the red edge of the lumi-F band.

ously observed by Eilfeld and Rüdiger at −140 °C (lumi-F, 673 nm) and by Pratt and Butler at −150 °C (FR_{660}, 660 nm). Meta-Fa was detected between −60 and −80 °C and was previously reported as A, FR′, and meta-F. All three intermediates were previously observed by Spruit et al. (1975) in their low-temperature flash photoreversion experiments. The difference spectra reported by Spruit et al. showed three absorption maxima that varied according to the temperature of irradiation and detection and the use of fresh or freeze-dried tissues.

The commonly accepted mechanism of photochromism for phytochrome is that photo- and thermal reversibilities of the phytochrome transformation involve two distinct pathways. To date, few studies show data that identify a common intermediate in the phytochrome forward (Pr → Pfr) and reverse (Pfr → Pr) pathways. At this stage, the possibility of a shared species can only be examined through spectral comparison of the intermediates in the photoreversion versus forward phototransformation reaction. A spectral comparison of our results with Pr → Pfr intermediates identified by Zhang et al. (1992) is most appropriate since data were collected on the same apparatus and experimental variations are minimal.

From the forward reaction, meta-Ra2, meta-Rac, lumi-R1, and lumi-R2 (data not shown) are distinctly different with respect to the major absorption bands (680−685 nm) of the reverse intermediates. In contrast, the absorption peak of meta-Ra1 is found at 664 nm, and as shown in Figure 7 the band is spectrally similar to those of lumi-F, meta-Fa, and meta-Fb. This comparison suggests that spectral convolution of lumi-F, meta-Fa, and/or meta-Fb can generate a spectrum similar to that of meta-Ra1. A common intermediate is not necessary and perhaps not expected when the roles of the intermediate species are considered. In the forward Pr → Pfr reaction, formation of the lumi-R1 and lumi-R2 species (Table 1) (Zhang et al., 1992; Björling et al., 1992) is associated with the *Z,Z,Z* to *Z,Z,E* chromophore configurational change. All meta intermediates that are subsequently formed have a *Z,Z,E* chromophore configuration. If meta-Ra1 is common between the two pathways, then meta-Ra1 and lumi-F, meta-Fa, and/or meta-Fb are expected to have similar chromophore−protein interactions. Upon going from Pfr to Pr, chromophore isomerization to form the *Z,Z,Z* configuration would then occur with decay of meta-Fa and/or meta-Fb, which is on a time scale considerably longer than what is expected for such an isomerization. If the configurational change from *Z,Z,E* to *Z,Z,Z* should occur in the early stages of the Pfr → Pr transformation, such as with lumi-F, then meta-Fa and meta-Fb should have a *Z,Z,Z* chromophore configuration, in contrast with meta-Ra1. These differences in chromophore configurations would argue against common intermediates.

In summary, TROD data were measured to examine the time dependence of the photoconversion of Pfr and Pr. Global analysis fits the TROD data to three exponential processes with lifetimes of 320 ns, 265 μs, and 5.5 ms. Comparison of these results with previous studies indicates that an unbranched sequential pathway can satisfactorily describe the processes observed in the TROD data. A spectral comparison of these intermediates indicates that only meta-Ra1 from the forward Pr → Pfr reaction shows spectral similarities to the intermediates from the reverse reaction, which could be a common step for the two pathways. However, the nature of these species supports two distinct pathways for the phytochrome phototransformation and photoreversion reactions.

ACKNOWLEDGMENT

We thank Jennifer L. Brooks (UCSC) for assistance with UV−vis measurements of Pfr and Pr.

REFERENCES

Björling, S. C., Zhang, C.-F., Farrens, D. L., Song, P.-S., & Kliger, D. S. (1992) *J. Am. Chem. Soc. 114*, 4581−4588.

Burke, M., Pratt, D. C., & Moscowitz, A. (1972) *Biochemistry 11*, 4025−4031.

Chai, Y. G., Song, P.-S., Cordonnier, M.-M., & Pratt, L. H. (1987) *Biochemistry 26*, 4947−4952.

Chen, E., Parker, W., Lewis, J. W., Song, P.-S., & Kliger, D. S. (1993) *J. Am. Chem. Soc. 115*, 9854−9855.

Cherry, J. R., Hondred, D., Keller, J. M., & Vierstra, R. D. (1991) in *Phytochrome Properties and Biological Actions* (Thomas, B., & Johnson, C., Eds.) NATO ASI Series H50, pp 113−126, Springer-Verlag, Berlin.

Cherry, J. R., Hondred, D., Walker, J. M., & Vierstra, R. D. (1992) *Proc. Natl. Acad. Sci. U.S.A. 89*, 5039−5043.

Eilfeld, P., & Rüdiger, W. (1985) *Z. Naturforsch. 40c*, 109−114.

Eilfeld, P., Eilfeld, P., Vogel, J., & Maurer, R. (1987) *Photochem. Photobiol. 45*, 825−830.

Farrens, D. L., Holt, R. E., Rospendowski, B. N., Song, P.-S., & Cotton, T. M. (1989) *J. Am. Chem. Soc. 111*, 9162−9169.

Farrens, D. L., Cordonnier, M.-M., Pratt, L. H., & Song, P.-S. (1992) *Photochem. Photobiol. 56*, 725−733.

Fodor, S. P. A., Lagarias, J. C., & Mathies, R. A. (1990) *Biochemistry 29*, 11141−11146.

Furuya, M., & Song, P.-S. (1994) in *Photomorphogenesis in Plants*, 2nd ed. (Kendrick, R. E., & Kronenberg, G. H. M., Eds.) pp 105−140, Kluwer Academic, Dordrecht, The Netherlands.

Goldbeck, R. A., & Kliger, D. S. (1993) in *Methods in Enzymology* (Riordan, J. F., & Vallee, B. L., Eds.) Vol. 226, pp 147−177, Academic Press, Orlando, FL.

Hahn, T. R., Song, P.-S., Quail, P. H., & Vierstra, R. D. (1984) *Plant Physiol. 74*, 755−758.

Henry, E. R., Hofrichter, J. (1992) in *Methods in Enzymology* (Brand, L., & Johnson, M., Eds.) Vol. 110, pp 129−192, Academic Press, Orlando, FL.
Hershey, H. P., Barker, R. F., Idler, K. B., Lissemore, J. L., & Quail, P. H. (1985) *Nucleic Acids Res. 13*, 8543−8559.
Hildebrandt, P., Hoffman, A., Lindemann, P., Heibel, G., Braslavsky, S. E., Schaffner, K., & Schrader, B. (1992) *Biochemistry 31*, 7957−7962.
Kandori, H., Yoshihara, K., & Tokutomi, S. (1992) *J. Am. Chem. Soc. 114*, 10958−10959.
Kendrick, R. E., & Spruit, C. J. P. (1973) *Photochem. Photobiol. 18*, 153−159.
Kendrick, R. E., & Spruit, C. J. P. (1977) *Photochem. Photobiol. 26*, 201−214.
Laemmli, U. K. (1970) *Nature (London) 227*, 680−685.
Lagarias, J. C., & Rapoport, H. (1980) *J. Am. Chem. Soc. 102*, 4821−4828.
Lapko, V. N., & Song, P.-S. (1995) *Photochem. Photobiol. 62*, 194−198.
Linschitz, H., Kasche, V., Butler, W. L., & Siegelman, H. W. (1966) *J. Biol. Chem. 241*, 3395−3403.
Ono, T., Shichida, Y., & Yoshizawa, T. (1986) *Photochem. Photobiol. 43*, 285−289.
Parker, W., Partis, M., & Song, P.-S. (1992) *Biochemistry 31*, 9413−9420.
Pratt, L. H., & Butler, W. L. (1968) *Photochem. Photobiol. 8*, 477−485.
Quail, P. H., Boylan, M., Parks, B. M., Short, T. W., & Wagner, D. (1995) *Science 268*, 675−680.
Rüdiger, W. (1987) *Photobiochem. Photobiophys. (Suppl. 1987)*, 217−227.
Rüdiger, W. (1992) *Photochem. Photobiol. 56*, 725−733.
Rüdiger, W., Thümmler, F., Cmiel, E., & Schneider, S. (1983) *Proc. Natl. Acad. U.S.A. 80*, 6244−6248.
Savikhin, S., Wells, T., Song, P.-S., & Struve, W. S. (1993) *Biochemistry 32*, 7512−7518.
Singh, B. R., Choi, J., Kwon, T., & Song, P.-S. (1989) *J. Biochem. Biophys. Methods 18*, 135−148.
Spruit, C. J. P., & Kendrick, R. E. (1977) *Photochem. Photobiol. 26*, 133−138.
Spruit, C. J. P., Kendrick, R. E., & Cooke, R. J. (1975) *Planta (Berlin) 127*, 121−132.
Stockhaus, J., Nagatani, A., Halfter, U., Kay, S., Furuya, M., & Chua, N.-H. (1992) *Genes Dev. 6*, 2364−2372.
Vierstra, R. D., & Quail, P. H. (1983) *Biochemistry 22*, 2498−2505.
Zhang, C.-F., Farrens, D. L., Björling, S. C., Song, P.-S., & Kliger, D. S. (1992) *J. Am. Chem. Soc. 114*, 4569−4580.

BI952115Z